



Artificial lithium fluoride surface coating on silicon negative electrodes for the inhibition of electrolyte decomposition in lithium-ion batteries: visualization of solid electrolyte interphase by in-situ AFM

Journal:	<i>Nanoscale</i>
Manuscript ID	NR-ART-07-2018-005354.R1
Article Type:	Paper
Date Submitted by the Author:	28-Aug-2018
Complete List of Authors:	Haruta, Masakazu; Doshisha University, Organization for Research Initiatives and Development Kijima, Yuki; Doshisha University Hioki, Ryuya; Doshisha University Doi, Takayuki; Doshisha University, Department of Molecular Chemistry and Biochemistry Minoru, Inaba; Faculty of Science and Engineering, Doshisha University



Journal Name

ARTICLE

Artificial lithium fluoride surface coating on silicon negative electrodes for the inhibition of electrolyte decomposition in lithium-ion batteries: visualization of solid electrolyte interphase by in-situ AFM †

Received 00th January 20xx,
Accepted 00th January 20xx

DOI: 10.1039/x0xx00000x

www.rsc.org/

Masakazu Haruta,* Yuki Kijima, Ryuya Hioki, Takayuki Doi and Minoru Inaba

The solid electrolyte interphase (SEI), which is a surface layer formed on the negative electrode, plays an important role in inhibiting the reductive decomposition of the electrolyte solution in a lithium-ion battery. However, it has not been understood well which components are important for SEI to prevent the electrolyte decomposition. Lithium fluoride (LiF), as an artificial SEI, was formed on an amorphous-Si thin film by physical vapor deposition. Changes in the surface morphology of the Si electrode with potential sweeping were investigated by in-situ atomic force microscopy (AFM). Although large numbers of non-uniform surface deposits that originate from electrolyte decomposition emerged on the bare Si-film electrode during the first lithiation process, few surface deposits were observed on the LiF-coated Si film electrode even after two cycles in an ethylene carbonate-based electrolyte solution without additives. It is clear that LiF is a required SEI component that inhibits the electrolyte decomposition on Si negative electrodes.

Introduction

The use of silicon as a negative-electrode material in lithium-ion batteries (LIBs) is a very promising method for realizing advanced secondary batteries with high energy densities because Li-Si alloys possess a high gravimetric and volumetric capacity (3578 mAh g⁻¹ and 2194 mAh cm⁻³, respectively, for Li₁₅Si₄) and operate at relatively low discharge potentials (~0.5 V vs. Li/Li⁺ on average).¹⁻⁵ Poor cyclability resulting from the pulverization of Si active materials due to large volume changes that occur during charge/discharge cycling has been a serious problem; however, recent studies using nanosized Si particles that reduce physical stress have overcome this problem.⁶⁻¹⁵ Furthermore, the formation of a solid state interphase (SEI) on the negative electrode in a LIB is necessary for it to operate in a stable manner during charging and discharging.¹⁶⁻²⁰

An SEI layer is formed by the deposition of the reductive-decomposition products of the electrolyte solution on the negative-electrode surface. The SEI layer plays a crucial role that prevents further electrolyte decomposition owing to its electron-insulating and ion-conducting features. Because the electrochemical properties of negative electrodes are strongly affected by the nature of the SEI, much effort has been directed toward understanding the chemistry, physical properties, and

formation mechanisms of SEIs, mainly on graphite negative electrodes, since the early stages of LIB development. Studies using X-ray photoelectron, Fourier-transform infrared, and Raman spectroscopies have provided high levels of insight into the chemical compositions of SEI-surface species.²¹⁻²⁸ Moreover, the surface morphologies of SEIs have been investigated by scanning and transmission electron microscopies (SEM and TEM).^{21-26,28,29} Due to these studies, that span over 30 years, significant knowledge in SEI has accumulated. An SEI layer that originates from a conventional carbonate-based electrolyte consists of a complex mixture of inorganic and organic species (LiF, Li₂O, and Li₂CO₃, (etc.), and lithium alkyl carbonates, lithium alkoxides, and polyethylene oxides (etc.), respectively).^{28,30,31}

While these SEI studies have provided rich information, inaccuracies still remain because most studies relied on ex-situ instrumentation and were conducted under operating conditions different from those of actual batteries. For example, the delicate SEI is subject to changes that are artefacts of sample handling and preparation (cell-disassembly and rinsing processes), and exposure to ambient conditions (air and vacuum) during ex-situ analyses. On the other hand, the surface morphology of a target electrode immersed in an electrolyte solution can be directly probed in real time using in-situ atomic force microscopy (AFM) coupled with electrochemical measurements.^{27,32-35} Moreover, high-resolution height profiles can be obtained by AFM in contrast to the two-dimensional projections provided by SEM and TEM. Therefore, in-situ AFM is a powerful tool that can aid in our understanding of the SEI-formation process associated with potential changes.

Doshisha University, Tatara-Miyakodani, Kyotanabe, Kyoto 610-0321, Japan. E-mail: mharuta@mail.doshisha.ac.jp

† Electronic Supplementary Information (ESI) available: See DOI: 10.1039/x0xx00000x

Although many types of SEI models have been proposed that are based on various analytical results,^{16,19,36,37} the essential role of each SEI component on electrochemical properties has not yet been clarified due to the complexity of the SEI structure. Therefore, improving electrochemical performance by providing guidance that leads to good SEIs with appropriate components is difficult. It is widely known that the addition of SEI-forming additives is a very effective way of improving the cyclability of negative electrodes, such as graphite and Si. For example, the addition of fluoroethylene carbonate (FEC) to an electrolyte remarkably improves the capacity retentions and the Coulombic efficiencies of graphite and Si negative electrodes. The resulting SEI layers have been reported to be rich in LiF as well as lithium carbonate and poly(FEC).^{28,38–40} Formation of LiF may hinder the Li⁺ transportation between the electrode and electrolyte due to the poor ionic conductivity of LiF,²¹ but on the other hand, fast Li⁺ transportations due to the presence of LiF have been reported.^{41,42} Moreover, an ab initio study of the decomposition mechanism of FEC indicated a glue effect by LiF on organic SEI components.⁴³ The importance of LiF as an SEI component has been highlighted by many researchers; however, the effects of LiF on the interfacial reactions between the electrolyte and electrode are not yet fully understood. In this study, we investigated electrolyte decomposition and SEI formation on model Si-thin-film electrodes by in-situ AFM. Furthermore, in order to understand the role of LiF as an SEI component, we formed artificial LiF layers on Si thin films.

Experimental

A 100-nm-thick Si thin film was deposited by RF magnetron sputtering (Kenix Co., Ltd.) on Cu foil at room temperature. An RF power of 1.5 W cm⁻² under an Ar pressure of 5.0 Pa was used to prepare amorphous Si devoid of any crystalline phase; these conditions were optimized in separate experiments. LiF layers were sequentially deposited on the Si thin film by RF sputtering at an RF power and an Ar pressure of 7.9 W cm⁻² and 2.0 Pa, respectively; thickness was controlled to be in the 2–16 nm range by adjusting the deposition time. The amorphous structure of the as-deposited Si film was confirmed by Raman spectroscopy (Fig. S1 in the EIS†). Following deposition, the Si film was transferred to an Ar-filled glovebox without exposure to air. A coin-type half-cell (CR2032) was assembled with the Si film as the working electrode, a separator (Celgard® 2400), and Li foil as a counter electrode. A solution of 1 M LiPF₆ in a mixture of ethylene carbonate (EC) and diethyl carbonate (DEC) (Battery Grade, UBE Industries, Ltd.) was used as the electrolyte solution; 10 wt.% FEC (Kishida Chemical) was added to the electrolyte as the SEI-forming additive. Charge and discharge testing was conducted at 30°C. The electrode was charged (lithiated) at C/2 to 20 mV, where it was maintained until the current decayed to a value of C/10, and then discharged (delithiated) at C/2 to 1.5 V. A three-electrode cell composed of the Si film as the working electrode, and Li counter and reference electrodes, was used for electrochemical impedance spectroscopy (EIS). Impedance spectra were obtained at 0.1 V on the charging process by applying an AC

voltage of 5 mV over the 0.03 Hz–300 kHz frequency range using a potentiostat/galvanostat equipped with a frequency-response analyzer (SP-150, Biologic).

In-situ AFM coupled with cyclic voltammetry (CV) was performed using an Agilent Technologies 5500 microscope equipped with a sample stage designed for electrochemical measurements; the instrument was operated in an Ar-filled glovebox (Miwa, 1ADB2 Special). The Si thin film (100 nm), with and without a 4-nm LiF layer, was deposited on a mirror-polished Cu substrate (Fig. S2†) and used as the working electrode, and the two Li wires used as counter and reference electrodes were immersed in the electrolyte solution containing 1 M lithium bis(trifluoromethane sulfonyl)imide (LiTFSI, Solvay) in EC+DEC (Kishida Chemical), where LiTFSI was used instead of LiPF₆ to circumvent the corrosion of the AFM components by HF. The water content in the electrolyte was confirmed to be lower than 20 ppm by Karl-Fischer titration (MKC-610, Kyoto Electronics Manufacturing Co., Ltd.). AFM was conducted in conventional contact mode using a Si₃N₄ cantilever (spring constant: 0.02 N m⁻¹) at room temperature. Typically, a 5 × 5 μm² image was obtained at a scan rate of 0.7 lines/s and a resolution of 512 points/line. A potentiostat/galvanostat (SP-200, Biologic) was used to scan the potential between 1.9 and 0.02 V at a constant sweep rate of 0.5 mV s⁻¹.

Results and discussion

Figure 1 displays discharge capacities and Coulombic efficiencies of amorphous-Si thin-film electrodes in 1 M LiPF₆/EC+DEC, with and without 10-wt.% FEC, as functions of cycle number. The discharge capacity of the Si film in the absence of FEC was initially 2800 mAh g⁻¹, but dropped to half this value at the 100th cycle. Cyclability was remarkably improved by the addition of FEC, with 91% of the initial capacity retained at the 300th cycle (2500 mAh g⁻¹ @300th). The Coulombic efficiency was also improved by the addition of FEC, and was 99% after 30 cycles. This improved performance

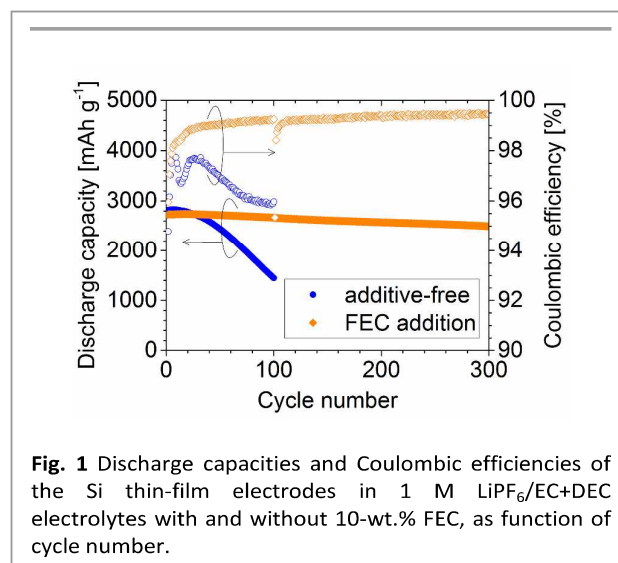
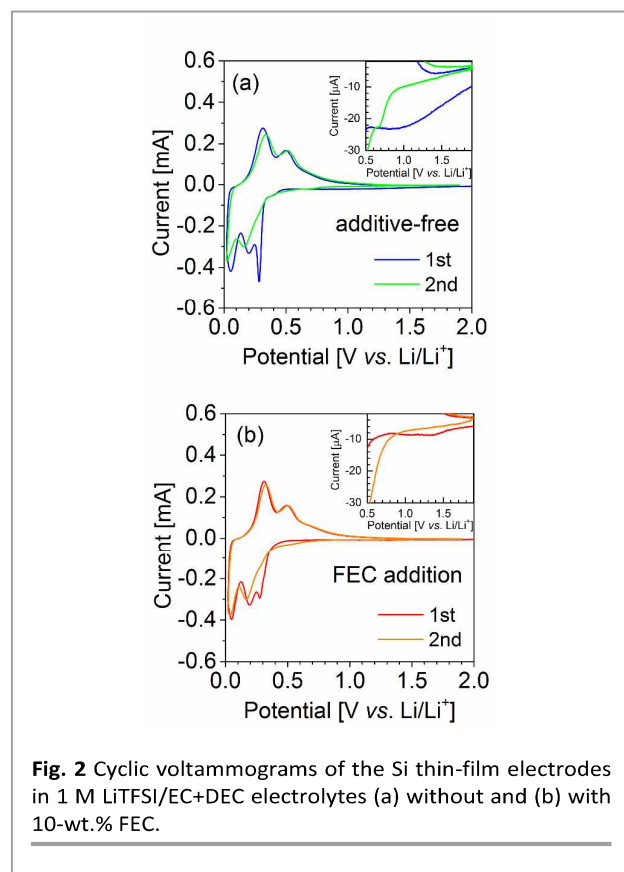


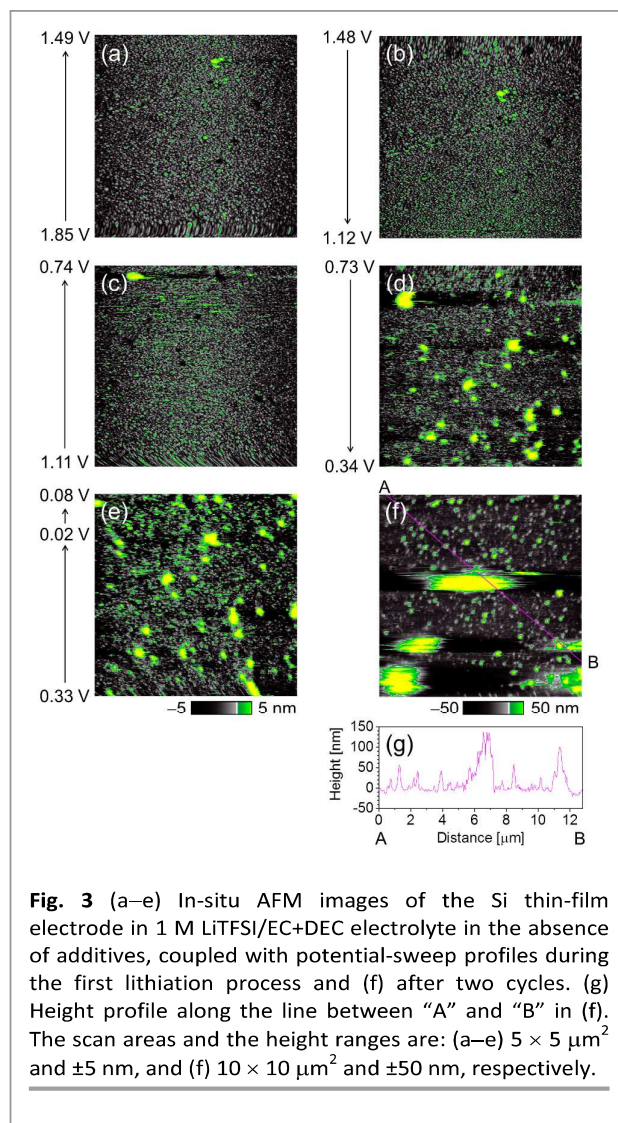
Fig. 1 Discharge capacities and Coulombic efficiencies of the Si thin-film electrodes in 1 M LiPF₆/EC+DEC electrolytes with and without 10-wt.% FEC, as function of cycle number.



is attributable to the formation of an effective SEI derived from FEC-decomposition products.

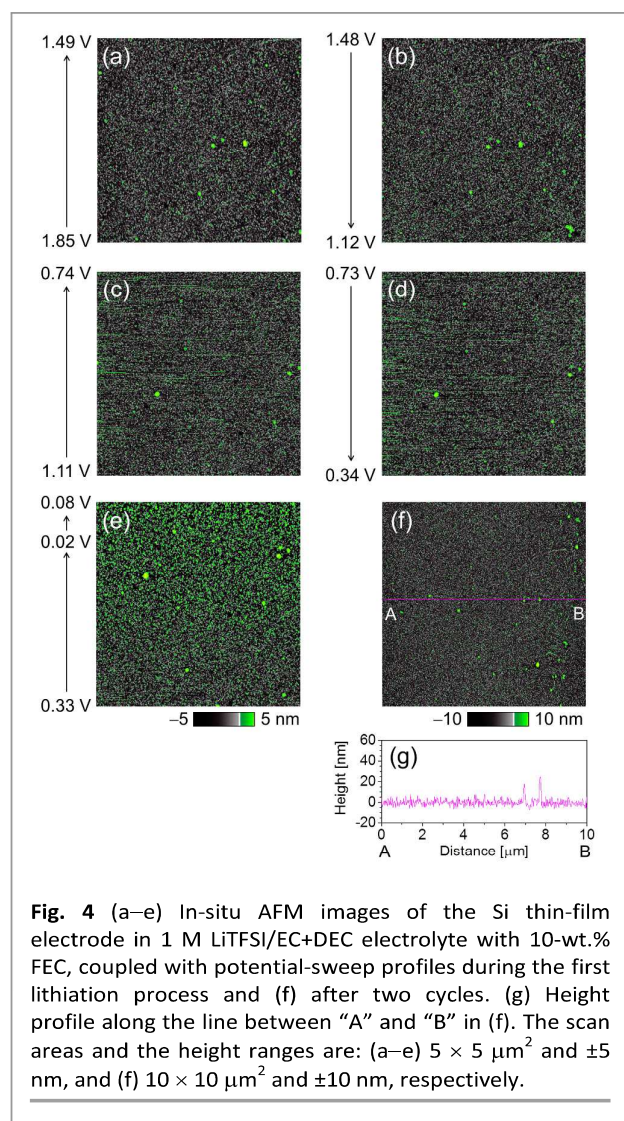
Figure 2a shows cyclic voltammograms (CV curves) of the Si-film electrode in 1 M LiTFSI/EC+DEC without additives using the in-situ AFM cell. A small cathodic current began to flow at about 2 V in the first cycle, and a small cathodic current peak arose at around 0.9 V, as shown in the inset of Fig. 2a. The cathodic current in this potential range was suppressed in the second cycle, indicating that the current in the first cycle was consumed by the irreversible reductive decomposition of the electrolyte and the formation of an SEI on the Si film. As the potential was swept to more negative values, cathodic current peaks appeared at 0.28, 0.20, and 0.05 V, which are assigned to Li-Si alloying reactions.^{2,44} Corresponding anodic current peaks were observed at 0.50 and 0.31 V, which are assigned to the dealloying reactions of Li-Si. It is plausible that the cathodic peak at 0.28 V and a barely discernible shoulder at around 0.39 V were caused by the irreversible consumption of Li^+ by dangling bonds in the amorphous-Si and the reductive reaction of Si oxides, respectively.^{44,45}

CV curves of the Si film electrode in the FEC-added electrolyte are shown in Fig. 2b. Although the shapes of the CV curves are very similar to those obtained without FEC, the cathodic current in the 2.0 to 0.9 V range was much smaller, even in the first cycle. A small peak was observed at around 1.4 V in the higher potential region, as shown in the inset of Fig. 2b, which is due to the reductive decomposition of FEC and the formation of a FEC-derived SEI. Owing to the formation of the



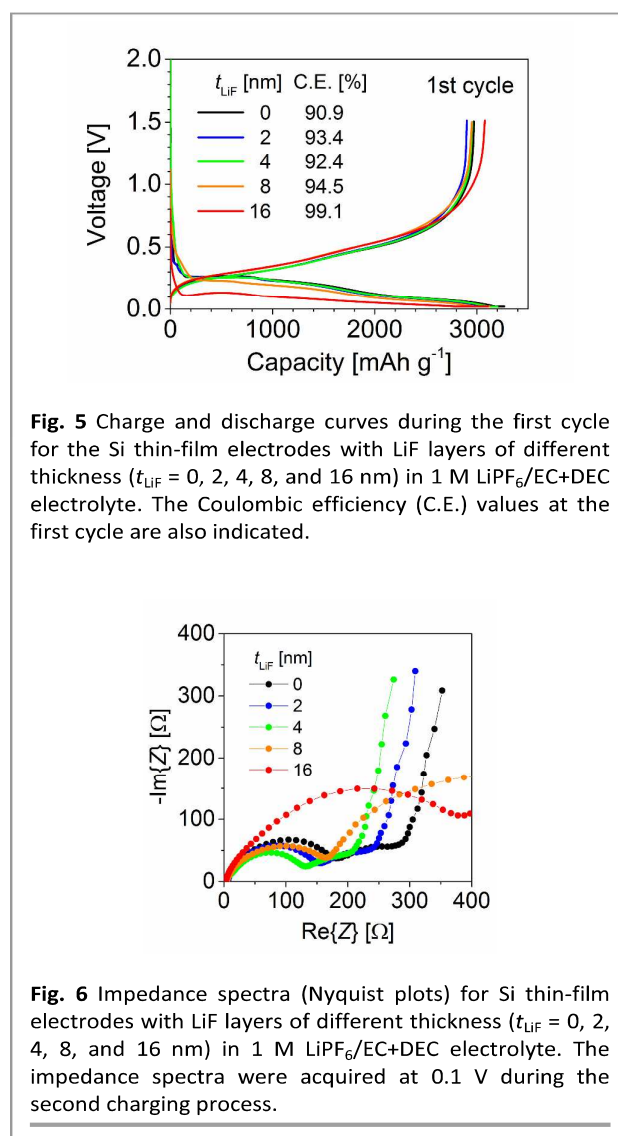
FEC-derived SEI, further reductive decomposition of the electrolyte was inhibited; hence the cathodic current at around 0.9 V, which was observed in the FEC-free electrolyte, was suppressed when FEC was added to the electrolyte.

The as-deposited Si thin film was composed of small grains several tens of nanometers in size, with a relatively flat surface except for some large precipitates and polishing flaws associated with the Cu substrate (Fig. S3[†]). In-situ AFM images ($5 \times 5 \mu\text{m}^2$) of the Si-film electrode obtained during the first lithiation process in the additive-free electrolyte are shown in Figs. 3a–e. No topological changes were observed during cathodic sweep down to 1.3 V. Higher regions in the AFM image (indicated in green to yellow) appeared at potentials lower than 1.2 V and their numbers increased with decreasing potential (Fig. 3b), indicating that deposits were generated on the Si surface. Sudden changes, which appear to correspond to line noise, appeared at potentials below 0.9 V (Fig. 3c). This phenomenon corresponds to the small cathodic current peak observed by CV in Fig. 2a. The surface deposits grew due to



intense electrolyte decomposition at potentials lower than 0.7 V (Fig. 3d). At potentials lower than 0.3 V (Fig. 3e), Si grains were observed to expand owing to Li-Si alloying, which roughened the surface. An AFM image ($10 \times 10 \mu\text{m}^2$) and a line height profile of the Si film electrode after two cycles are shown in Figs. 3f and 3g, respectively. Inhomogeneous surface deposits were demonstrated on the Si film; local large aggregates of decomposition products, with lateral dimensions and heights of several micrometers and over 100 nm, respectively, were formed. These inhomogeneous deposits resulted in the non-uniform alloying of Li to the Si active material during lithiation, and thus the resulting non-uniform volume changes degraded the Si electrode rapidly as shown in Fig. 1.

Figures 4a–e displays in-situ AFM images of the Si-film electrode in the FEC-added electrolyte during the first lithiation process. In contrast to the morphological changes observed in the absence of FEC (Fig. 3), many fewer topological changes were observed on the Si film in the presence of FEC, although



line noise appeared in the 1.1 to 0.3 V range (Figs. 4c and 4d). We believe that a homogeneous SEI layer, formed from FEC-reduction products at high potentials of around 1.4 V, inhibited electrolyte decomposition at lower potentials. At potentials below 0.3 V (Fig. 4e), Si-grain expansion, which is attributed to the alloying reaction, was clearly observed due to smaller amounts of surface deposits. The surface of the Si-film electrode after two cycles (Fig. 4f) was clearly much flatter in the presence of FEC than in its absence (Fig. 3f), and the roughness of the surface was within $\pm 10 \text{ nm}$, with the exception of some precipitates, as shown in Fig. 4g.

SEI layers derived from FEC have been reported to contain large amounts of LiF.^{28,38-40} In order to understand the effects of LiF, as an SEI component, on electrochemical properties, we prepared artificial LiF layers of different thicknesses ($t_{\text{LiF}} = 0, 2, 4, 8,$ and 16 nm) on Si-film electrodes. The values of t_{LiF} for 8 and 16 nm were determined by cross-sectional SEM, and the others were estimated from the deposition time. The LiF layer grew in island-growth mode during film deposition;⁴⁶ a

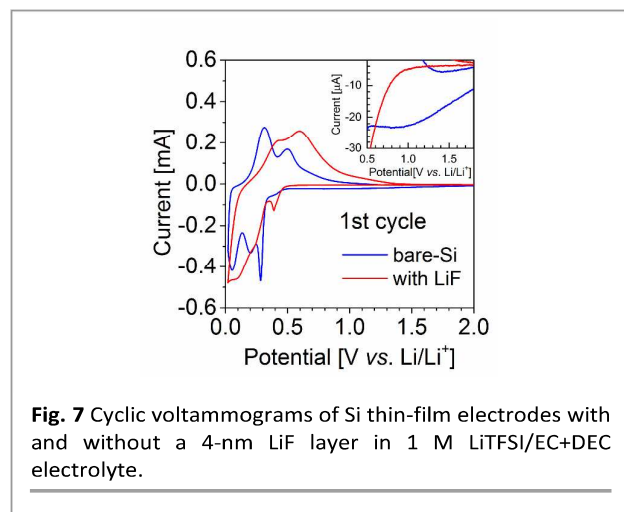


Fig. 7 Cyclic voltammograms of Si thin-film electrodes with and without a 4-nm LiF layer in 1 M LiTFSI/EC+DEC electrolyte.

continuous LiF film was considered to have formed at t_{LiF} values greater than ~ 8 nm of t_{LiF} in this study using the non-polished Cu foil substrate. The LiF coverage on the Si film would influence ion transportation between the electrolyte and the Si electrode. Charge and discharge characteristics during the first cycle for the LiF-coated Si-film electrodes are shown in Fig. 5. Monotonous changes in potential on charging and discharging, without any clear potential plateaus, were observed, which indicate the absence of crystalline $\text{Li}_{15}\text{Si}_4$ -phase formation.^{47,48} The charge and discharge curves were almost unchanged by the presence of LiF layers up to a thickness of 8 nm. However, the 16-nm LiF-coated electrode exhibited large polarization owing to the low ionic conductivity of LiF. The discharge capacity of each electrode at the first cycle was ~ 3000 mAh g^{-1} ; therefore, the influence of the LiF layer on the discharge capacity was negligible. While Coulombic efficiency of the Si film at the first cycle was 90.9% in the absence of LiF, it increased with increasing LiF thickness and was 99.1% for the 16-nm LiF-coated electrode. The high Coulombic efficiency was the result of the effective suppression of electrolyte decomposition by the LiF layer on the Si-film electrode.

The Coulombic efficiencies during the initial cycles increased as a consequence of the LiF-coating; however, the retained capacities of the LiF-coated Si electrodes were not appreciably improved from that of the bare-Si electrode (Fig. S4†) and were clearly inferior to that of the bare-Si electrode when FEC was added (Fig. 1). The SEI layer originating from FEC-reduction products is capable of enduring certain morphological changes of the Si film during charge/discharge cycling through elastic deformations that are due to flexible organic polymers in addition to LiF. On the other hand, the LiF-coating layer is brittle and hence easily cracked during cycling, leading to electrolyte decomposition on the newly exposed Si surface and poor capacity retention.

Impedance spectra (Nyquist plots) acquired at 0.1 V during the second charging process for the Si-film electrodes with LiF coatings of different thicknesses are shown in Fig. 6. Each impedance spectrum consisted of two semi-circles in the higher

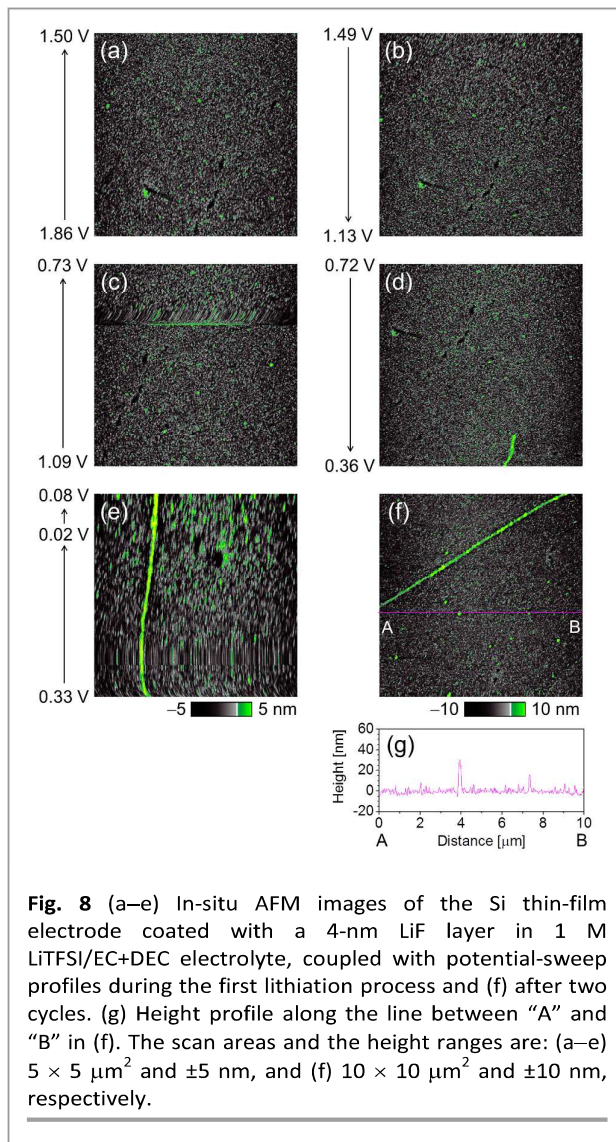


Fig. 8 (a–e) In-situ AFM images of the Si thin-film electrode coated with a 4-nm LiF layer in 1 M LiTFSI/EC+DEC electrolyte, coupled with potential-sweep profiles during the first lithiation process and (f) after two cycles. (g) Height profile along the line between “A” and “B” in (f). The scan areas and the height ranges are: (a–e) $5 \times 5 \mu\text{m}^2$ and ± 5 nm, and (f) $10 \times 10 \mu\text{m}^2$ and ± 10 nm, respectively.

and lower frequency regions, which are assigned to the impedances of the SEI layer and the charge-transfer reaction, respectively.^{24,49} The SEI resistance of the 16-nm LiF-coated Si film was much higher than that of the bare-Si film due to the low ionic conductivity of LiF. However, LiF coatings thicknesses ≤ 8 nm provided SEI resistances lower than that of the uncoated Si film; the lowest SEI resistance was obtained at a LiF thickness of 4 nm. The observed decrease in SEI resistance implies that the LiF layer effectively inhibited electrolyte decomposition and suppressed the formation of a thick SEI. Furthermore, the co-existence of LiF and oxides derived from electrolyte-decomposition products, such as Li_2CO_3 , resulted in improved ion conductivity at the interfaces between LiF and the oxides.^{42,50} The lack of electronic conductivity of LiF and the enhanced ionic conductivity at the LiF/oxide interface are favorable SEI features, and their synergism led to a high Coulombic efficiency and a low interfacial impedance. We believe that optimization of the

thickness (amount) of LiF taking into account the type of electrolyte is important to achieve the low interfacial impedance.

Figure 7 compares the first CV curves of the Si-film electrodes, with and without a 4-nm LiF layer, in 1 M LiTFSI/EC+DEC. It should be noted that the Si surface was covered with LiF with a high coverage in comparison with those used for charge and discharge tests because a mirror-polished Cu substrate with a flat surface was used in the CV-coupled AFM. As shown in the inset in Fig. 7, the bare-Si film exhibited a broad cathodic peak at around 0.9 V, which originates from electrolyte decomposition, as discussed earlier (Fig. 2a). However, the cathodic current at around 0.9 V was not observed for the LiF-coated Si film. The cathodic and anodic current peaks for the LiF-coated Si film, assigned to the alloying and de-alloying reactions, respectively, shifted to lower and higher potentials, respectively, compared to those of the bare-Si film, indicating that the LiF layer caused an increment of the polarization. The Coulombic efficiencies derived from CV for the Si electrodes with and without LiF coating were 92% and 65%, respectively.

In-situ AFM images of the LiF-coated Si-film electrode in 1 M LiTFSI/EC+DEC are summarized in Fig. 8. No significant topological changes were observed on the Si surface down to 0.3 V during the first cathodic potential sweep (Figs. 8a-d). Si grains were observed to expand below 0.3 V owing to lithiation reactions (Fig. 8e, unfortunately, this image was strongly affected by drift during AFM scanning). Few surface deposits were observed even after two cycles (Fig. 8f), and the surface roughness of the LiF-coated Si electrode was very low, within ± 10 nm, except for the presence of some precipitates (Fig. 8g). The flat surface of the LiF-coated Si film was also confirmed by surface analyses based on the root-mean-square roughness (Fig. S5). It should be noted that FEC was not added to the electrolyte solution depicted in Fig. 8; nevertheless, the formation of surface deposits was strongly suppressed, as was observed when FEC was added to the electrolyte (Fig. 4). These results revealed that the LiF layer on the Si electrode prevents electrolyte decomposition; hence LiF is a very important SEI-layer component. Although the electrolyte decomposition was inhibited by the LiF layer, the cyclability of the LiF-coated Si electrodes was improved little due to cracking of the LiF layers as mentioned above. Therefore, we conclude that not only LiF, but also flexible components, such as organic polymers that can accommodate volume changes of the Si active material during charge/discharge cycling, are required as SEI components in order to achieve improved cyclability for Si negative electrodes.

Conclusions

The SEI growth process on an amorphous-Si thin-film electrode in 1 M LiTFSI/EC+DEC electrolyte was investigated by in-situ AFM coupled with CV. Surface deposits on the Si-film electrode formed below 1.2 V during the first cathodic potential sweep; these deposits grew with decreasing potential in the additive-free electrolyte. Owing to the reductive decomposition

of the electrolyte, a non-uniform SEI was formed on the Si surface, which led to poor cycling performance due to inhomogeneous volume changes of the Si active material.

In contrast, the surface morphology of the Si-film electrode was almost unchanged in the FEC-added electrolyte during potential sweeping, with the exception of volume changes in the Si grains at lower potentials, indicating that the SEI layer derived from FEC-reduction products effectively inhibited electrolyte decomposition.

In order to understand the effects of LiF, which is one of the main components produced during the decomposition of FEC, thin artificial LiF layers of different thickness were formed on Si-film electrodes. Uniform surfaces with small amounts of deposits were observed for the Si film coated with LiF after two cycles in the additive-free electrolyte. Moreover, the LiF-coated Si-film electrodes exhibited improved Coulombic efficiencies during the initial cycles. These observations strongly suggest that LiF is an important component that prevents electrolyte decomposition on Si negative electrodes. The surface layers of Si electrodes, which consist of electronically non-conductive LiF and ionically conductive LiF/oxide interfaces, works as favorable SEIs. Unfortunately the LiF layer did not improve Si-film capacity retention; we believe that, in addition to inorganic LiF, organic SEI components are also required in order to achieve Si negative electrodes with long cycle lives.

Conflicts of interest

There are no conflicts to declare.

Acknowledgements

This research was supported by the Japan Science and Technology Agency (JST) ALCA-SPRING and the Japan Society for the Promotion of Science (JSPS) KAKENHI Grant Number 16H04649.

Notes and references

- 1 B. A. Boukamp, G. C. Lesh, R. A. Huggins, All - Solid Lithium Electrodes with Mixed - Conductor Matrix, *J. Electrochem. Soc.*, 1981, **128**, 725-729.
- 2 R.A. Huggins, Lithium alloy negative electrodes, *J. Power Sources* 1999, **81**, 13-19.
- 3 U. Kasavajjula, C. Wang, A. J. Appleby, Nano- and bulk-silicon-based insertion anodes for lithium-ion secondary cells, *J. Power Sources*, 2007, **163**, 1003-1039.
- 4 D. Larcher, S. Beattie, M. Morcrette, K. Edström, J-C. Jumas, J-M. Tarascon, Recent findings and prospects in the field of pure metals as negative electrodes for Li-ion batteries, *J. Mater. Chem.*, 2007, **17**, 3759-3772.
- 5 H. Wu, Y. Cui, Designing nanostructured Si anodes for high energy lithium ion batteries, *Nano Today*, 2012, **7**, 414-429.
- 6 H. Li, X. Huang, L. Chen, Z. Wu, Y. Liang, A High Capacity Nano-Si Composite Anode Material for Lithium Rechargeable Batteries, *Electrochem. Solid-State Lett.*, 1999, **2**, 547-549.
- 7 H. Kim, M. Seo, M-H. Park, J. Cho, A Critical Size of Silicon Nano-Anodes for Lithium Rechargeable Batteries, *Angew. Chem. Int. Ed.*, 2010, **49**, 2146-2149.

- 8 C. K. Chan, H. L. Peng, G. Liu, K. McIlwrath, X. F. Zhang, R. A. Huggins, Y. Cui, High-performance lithium battery anodes using silicon nanowires, *Nat. Nanotechnol.*, 2008, **3**, 31-35.
- 9 M-H. Park, M. G. Kim, J. Joo, K. Kim, J. Kim, S. Ahn, Y. Cui, J. Cho, Silicon Nanotube Battery Anodes, *Nano Lett.*, 2009, **9**, 3844-3847.
- 10 H. Wu, G. Chan, J. W. Choi, I. Ryu, Y. Yao, M. T. McDowell, S. W. Lee, A. Jackson, Y. Yang, L. Hu, Y. Cui, Stable cycling of double-walled silicon nanotube battery anodes through solid-electrolyte interphase control, *Nature Nanotech.*, 2012, **7**, 310-215.
- 11 L. Y. Beaulieu, K. W. Ebrman, R. L. Turner, L. J. Krause, J. R. Dahn, Colossal Reversible Volume Changes in Lithium Alloys, *Electrochim. Solid-State Lett.*, 2001, **4**, A137-A140.
- 12 J. P. Maranchi, A. F. Hepp, P. N. Kumta, High Capacity, Reversible Silicon Thin-Film Anodes for Lithium-Ion Batteries, *Electrochim. Solid-State Lett.*, 2003, **6**, A198-A201.
- 13 T. Takamura, S. Ohara, M. Uehara, J. Suzuki, K. Sekine, A vacuum deposited Si film having a Li extraction capacity over 2000 mAh/g with a long cycle life, *J. Power Sources*, 2004, **129**, 96-100.
- 14 M. Saito, K. Nakai, T. Yamada, T. Takenaka, M. Hirota, A. Kamei, A. Tasaka, M. Inaba, Si thin platelets as high-capacity negative electrode for Li-ion batteries, *J. Power Sources*, 2011, **196**, 6637-6643.
- 15 M. Haruta, R. Hioki, T. Moriyasu, A. Tomita, T. Takenaka, T. Doi, M. Inaba, Morphology changes and long-term cycling durability of Si flake powder negative electrode for lithium-ion batteries, *Electrochimica Acta*, 2018, **267**, 94-101.
- 16 D. Aurbach, Review of selected electrode-solution interactions which determine the performance of Li and Li ion batteries, *J. Power Sources*, 2000, **89**, 206-218.
- 17 P. Verma, P. Maire, P. Novák, A review of the features and analyses of the solid electrolyte interphase in Li-ion batteries, *Electrochimica Acta*, 2010, **55**, 6332-6341.
- 18 R. Marom, S.F. Amalraj, N. Leifer, D. Jacob, D. Aurbach, A review of advanced and practical lithium battery materials, *J. Mater. Chem.*, 2011, **21**, 9938-9954.
- 19 M. Gauthier, T.J. Carney, A. Grimaud, L. Giordano, N. Pour, H. Chang, D.P. Fenning, S.F. Lux, O. Paschos, C. Bauer, F. Maglia, S. Lupart, P. Lamp, Y. Shao-Horn, Electrode-Electrolyte Interface in Li-Ion Batteries: Current Understanding and New Insights, *J. Phys. Chem. Lett.*, 2015, **6**, 4653-4672.
- 20 S.J. An, J. Li, C. Daniel, D. Mohanty, S. Nagpure, D.L. Wood, The state of understanding of the lithium-ion-battery graphite solid electrolyte interphase (SEI) and its relationship to formation cycling, *Carbon*, 2016, **105**, 52-76
- 21 A.M. Andersson, K. Edström, Chemical Composition and Morphology of the Elevated Temperature SEI on Graphite, *J. Electrochem. Soc.*, 2001, **148**, A1100-A1109.
- 22 H. Ota, Y. Sakata, A. Inoue, S. Yamaguchi, Analysis of Vinylene Carbonate Derived SEI Layers on Graphite Anode, *J. Electrochim. Soc.*, 2004, **151**, A1659-A1669.
- 23 K. Naoi, N. Ogihara, Y. Igarashi, A. Kamakura, Y. Kusachi, K. Utsugi, Disordered Carbon Anode for Lithium-Ion Battery I. An Interfacial Reversible Redox Action and Anomalous Topology Changes, *J. Electrochem. Soc.*, 2005, **152**, A1047-A1053.
- 24 L. Chen, K. Wang, X. Xie, J. Xie, Effect of vinylene carbonate (VC) as electrolyte additive on electrochemical performance of Si film anode for lithium ion batteries, *J. Power Sources*, 2007, **174**, 538-543.
- 25 D.E. Arreaga-Salas, A.K. Sra, K. Roodenko, Y.J. Chabal, C.L. Hinkle, Progression of Solid Electrolyte Interphase Formation on Hydrogenated Amorphous Silicon Anodes for Lithium-Ion Batteries, *J. Phys. Chem. C*, 2012, **116**, 9072-9077.
- 26 S. Bhattacharya, A.T. Alpas, Micromechanisms of solid electrolyte interphase formation on electrochemically cycled graphite electrodes in lithium-ion cells, *Carbon*, 2012, **50**, 5359-5371.
- 27 A.v. Cresce, S.M. Russell, D.R. Baker, K.J. Gaskell, K. Xu, In Situ and Quantitative Characterization of Solid Electrolyte Interphases, *Nano Lett.*, 2014, **14**, 1405-1412.
- 28 M. Nie, J. Demeaux, B.T. Young, D.R. Heskett, Y. Chen, A. Bose, J.C. Woicik, B.L. Lucht, Effect of Vinylene Carbonate and Fluoroethylene Carbonate on SEI Formation on Graphitic Anodes in Li-Ion Batteries, *J. Electrochem. Soc.*, 2015, **162**, A7008-A7014.
- 29 W. Märkle, C-Y. Lu, P. Novák, Morphology of the Solid Electrolyte Interphase on Graphite in Dependency on the Formation Current, *J. Electrochem. Soc.*, 2011, **158**, A1478-A1482.
- 30 K.W. Schroder, A.G. Dylla, S.J. Harris, L.J. Webb, K.J. Stevenson, Role of Surface Oxides in the Formation of Solid-Electrolyte Interphases at Silicon Electrodes for Lithium-Ion Batteries, *ACS Appl. Mater. Interfaces*, 2014, **6**, 21510-21524.
- 31 P. Lu, C. Li, E.W. Schneider, S.J. Harris, Chemistry, Impedance, and Morphology Evolution in Solid Electrolyte Interphase Films during Formation in Lithium Ion Batteries, *J. Phys. Chem. C*, 2014, **118**, 896-903.
- 32 M. Inaba, Z. Siroma, A. Funabiki, Z. Ogumi, Electrochemical Scanning Tunneling Microscopy Observation of Highly Oriented Pyrolytic Graphite Surface Reactions in an Ethylene Carbonate-Based Electrolyte Solution, *Langmuir*, 1996, **12**, 1535-1540.
- 33 S-K. Jeong, M. Inaba, T. Abe, Z. Ogumi, Surface Film Formation on Graphite Negative Electrode in Lithium-Ion Batteries: AFM Study in an Ethylene Carbonate-Based Solution, *J. Electrochem. Soc.*, 2001, **148**, A989-A993.
- 34 Y. Domi, M. Ochida, S. Tsubouchi, H. Nakagawa, T. Yamanaka, T. Doi, T. Abe, Z. Ogumi, In Situ AFM Study of Surface Film Formation on the Edge Plane of HOPG for Lithium-Ion Batteries, *J. Phys. Chem. C*, 2011, **115**, 25484-25489.
- 35 C. Shen, S. Wang, Y. Jin, W-Q. Han, In Situ AFM Imaging of Solid Electrolyte Interfaces on HOPG with Ethylene Carbonate and Fluoroethylene Carbonate-Based Electrolytes, *ACS Appl. Mater. Interfaces*, 2015, **7**, 25441-25447.
- 36 E. Peled, D. Golodnitsky, G. Ardel, Advanced Model for Solid Electrolyte Interphase Electrodes in Liquid and Polymer Electrolytes, *J. Electrochem. Soc.*, 1997, **144**, L208-L210.
- 37 E. Peled, S. Menkin, Review—SEI: Past, Present and Future, *J. Electrochem. Soc.*, 2017, **164**, A1703-A1719.
- 38 C.C. Nguyen, B.L. Lucht, Comparative Study of Fluoroethylene Carbonate and Vinylene Carbonate for Silicon Anodes in Lithium Ion Batteries, *J. Electrochem. Soc.*, 2014, **161**, A1933-A1938.
- 39 C. Xu, F. Lindgren, B. Philippe, M. Gorgoi, F. Björefors, K. Edström, T. Gustafsson, Improved Performance of the Silicon Anode for Li-Ion Batteries: Understanding the Surface Modification Mechanism of Fluoroethylene Carbonate as an Effective Electrolyte Additive, *Chem. Mater.*, 2015, **27**, 2591-2599.
- 40 I.A. Shkrob, J.F. Wishart, D.P. Abraham, What Makes Fluoroethylene Carbonate Different?, *J. Phys. Chem. C*, 2015, **119**, 14954-14964.
- 41 Y. Lu, Z. Tu, L.A. Archer, Stable lithium electrodeposition in liquid and nanoporous solid electrolytes, *Nat. Mater.*, 2014, **13**, 961-969.

ARTICLE

Journal Name

- 42 Q. Zhang, J. Pan, P. Lu, Z. Liu, M.W. Verbrugge, B.W. Sheldon, Y-T. Cheng, Y. Qi, X. Xiao, Synergetic Effects of Inorganic Components in Solid Electrolyte Interphase on High Cycle Efficiency of Lithium Ion Batteries, *Nano Lett.*, 2016, **16**, 2011-2016.
- 43 Y. Okuno, K. Ushirogata, K. Sodeyama, Y. Tateyama, Decomposition of the fluoroethylene carbonate additive and the glue effect of lithium fluoride products for the solid electrolyte interphase: an ab initio study, *Phys. Chem. Chem. Phys.*, 2016, **18**, 8643-8653.
- 44 E. Pollak, G. Salitra, V. Baranchugov, D. Aurbach, In Situ Conductivity, Impedance Spectroscopy, and Ex Situ Raman Spectra of Amorphous Silicon during the Insertion/Extraction of Lithium, *J. Phys. Chem. C*, 2007, **111**, 11437-11444.
- 45 H. Li, X. Huang, L. Chen, G. Zhou, Z. Zhang, D. Yu, Y.J. Mo, N. Pei, The crystal structural evolution of nano-Si anode caused by lithium insertion and extraction at room temperature, *Solid State Ionics*, 2000, **135**, 181-191.
- 46 M. Kumar, S.A. Khan, P. Rajput, F. Singh, A. Tripathi, K. Avasthi, A.C. Pandey, Size effect on electronic sputtering of LiF thin films, *J. Appl. Phys.*, 2007, **102**, 083510.
- 47 M.N. Obrovac, L. Christensen, Structural Changes in Silicon Anodes during Lithium Insertion/Extraction, *Electrochem. Solid State Lett.*, 2004, **7**, A93-A96.
- 48 T.D. Hatchard, J.R. Dahn, In situ XRD and electrochemical study of the reaction of lithium with amorphous silicon, *J. Electrochem. Soc.*, 2004, **151**, A838-A842.
- 49 A. Funabiki, M. Inaba, Z. Ogumi, S. Yuasa, J. Otsuji, A. Tasaka, Impedance study on the electrochemical lithium intercalation into natural graphite powder, *J. Electrochem. Soc.*, 1998, **145**, 172-178.
- 50 J. Pan, Q. Zhang, X. Xiao, Y-T. Cheng, Y. Qi, Design of Nanostructured Heterogeneous Solid Ionic Coatings through a Multiscale Defect Model, *ACS. Appl. Mater. Interfaces*, 2016, **8**, 5687-5693.

Artificial lithium fluoride surface coating on silicon negative electrodes for the inhibition of electrolyte decomposition in lithium-ion batteries: visualization of solid electrolyte interphase by in-situ AFM

Masakazu Haruta, Yuki Kijima, Ryuya Hioki, Takayuki Doi, Minoru Inaba

The surface deposition of reduced electrolytes on Si negative electrodes and its inhibition by an artificial coating were demonstrated by in-situ AFM.

